



Collection efficiency of fog events

Sonia Montecinos^{a,b,*}, Danilo Carvajal^{c,d}, Pilar Cereceda^e, Miguel Concha^f

^a Departamento de Física y Astronomía, Facultad de Ciencias, Universidad de La Serena, Avda. Juan Cisternas 1200, La Serena, Chile

^b Centro Estudio Recursos de Energía, Universidad Arturo Prat (CERE-UNAP), Iquique, Chile

^c Instituto de Investigación Multidisciplinario en Ciencia y Tecnología, Universidad de La Serena, Benavente 980, La Serena, Chile

^d International Organization for Dew Utilization (OPUR), 60 rue Emeriau, 75015 Paris, France

^e Centro del Desierto de Atacama, Pontificia Universidad Católica de Chile, Avda. Vicuña Mackenna 4860, Macul - Santiago, Chile

^f Departamento de Física y Astronomía, Facultad de Ciencias, Universidad de La Serena, Avda. Juan Cisternas 1200, La Serena, Chile



ARTICLE INFO

Keywords:

Fog collection efficiency

Fog

Fog microphysics

ABSTRACT

Fog is an important water resource, especially in arid and semi-arid zones. The usual method to collect fog water is placing a rectangular mesh perpendicular to the wind which traps fog droplets. The collector catches a fraction of the fog's water droplets, allowing them to grow by coalescence until large enough to fall by gravity for collection. Fog events can last from minutes to hours, or even longer. This study aimed to evaluate the efficiency (η) of a standard fog collector (SFC) to gather fog water. Efficiency is defined as the ratio between the water reaching the collector's gutter (CW) and the liquid water flux (LWF) normal to the collector's mesh, integrated in a period of time. After a fog event begins, mesh collectors require some time to reach saturation and begin dripping; further, the system does not achieve a stationary state at field conditions. Therefore, we considered entire fog events when evaluating efficiency. The CW was measured using a rain gauge, and the LWF was calculated based on the liquid water content (LWC) obtained through a fog droplet spectrometer, and data of wind velocity registered by a meteorological station. The duration of the analyzed events ranged from 20 min to 11 h 40 min. A lag of up to one hour between the arrival of fog and the beginning of the measured water output was observed. Both processes started simultaneously when preceded by another fog event.

For the analyzed events, η ranged between 0% and 36.8%. Isolated events of up to 30 minutes resulted in zero CW measurements because the mesh requires time to become saturated before dripping. Furthermore, η was zero if the mean dew point depression (DPD) was above 0.2 °C or the mean LWC was below 0.045 g m⁻³. We found that η decreases with increasing mean volume diameter (MVD) for MVD \gtrsim 10 μ m. Finally, η increased with wind speed for events in which the MVD > 12 μ m.

1. Introduction

In places where water is scarce, fog represents an important alternative water resource. Researchers have carried out many experiments around the world showing that it is possible to get enough water from fog to supply the water needs of villages and small towns (Klemm et al., 2012).

The most widely-used technology for collecting fog water is the large fog collector (LFC), a rectangular mesh placed perpendicular to wind flow. When exposed to a foggy environment, water droplets carried by the wind are pushed against the mesh and become trapped. After successive impacts, the droplets grow by coalescence until they are large enough to fall by gravity, and a gutter transports the water to a tank.

Fog collection involves several processes, each characterized by

their own efficiency:

- Aerodynamic collection efficiency is defined as the fraction of fog droplets in the unperturbed air flow that could potentially reach the mesh fibers. Rivera (2011) defines it as “the maximum fraction of the unperturbed fog that can be captured by the fog water collector”. Based on this definition, the maximum theoretical aerodynamic efficiency approaches the mesh shadow coefficient (SC), which occurs when the aerodynamic resistance of the collector tends to zero.
- Deposition efficiency refers to the droplets in a collision path with the mesh fibers. Some may actually become trapped by the fibers as a result of several mechanisms: interception, which is important when the incident droplets have a similar or larger diameter than the mesh fiber; diffusion (Brownian motion), which is relevant for

* Corresponding author at: Departamento de Física y Astronomía, Facultad de Ciencias, Universidad de La Serena, Avda. Juan Cisternas 1200, La Serena, Chile.
E-mail address: smontecinos@userena.cl (S. Montecinos).

small droplets ($< 0.1 \mu\text{m}$); and inertial impaction, which occurs when the droplets in the air stream do not follow the air stream around the collector but, because of their inertia, impact it. This process is important when the size of the droplets are much smaller than the mesh fiber. Impaction is the most relevant mechanism if fog droplets are between $5 \mu\text{m}$ and $50 \mu\text{m}$ and if the fiber has a width of one mm—which is the case for the Raschel mesh widely used in fog harvesting (Schatzmann, 1999; Park et al., 2013; Regalado and Ritter, 2016).

- After the two processes mentioned above, draining efficiency describes the fraction of fog water that reaches the final collection system (gutter). The droplets captured by the mesh can be lost due to two factors: re-entrainment of water to the air stream (Thorne et al., 1982) and dripping out of the gutter. The last effect results because plastic meshes experience bending due to the air flow, causing water droplets to fall outside the gutter.

Schemenauer and Joe (1989) analyzed the collection efficiency E_m of an LFC (12 m long \times 4 m height) equipped with a double Raschel mesh by measuring the LWC at the front and behind the LFC. Wind speed was measured 6 m above the ground (agl) in front of the fog collector, at the height of its centerline. To evaluate LWC, the authors used two Particle Measuring Systems Forward Scattering Spectrometer Probes (FSSP). E_m was calculated as the percentage difference between the LWC in front of and behind the LFC. The authors applied this methodology on 10 samples during fog events—not entire fog events—(Schemenauer R., personal communication, 2017) with a duration between 20 s and 300 s and found that it ranged between 27% and 69%. The authors further measured the flow of the water gathered by the final collection system, finding that the efficiency was 2.9 times less than that calculated with this methodology; therefore, the actual collection efficiency was near 20%.

To our knowledge, aside the article from Schemenauer and Joe (1989), there exist no studies about the efficiency of fog collectors in field conditions. Park et al. (2013) carried out experiments under controlled conditions (glove box) to measure the fog collection efficiency of different kinds of meshes, including the conventional Raschel mesh. Furthermore, some theoretical investigations on fog collection efficiency have been carried out (Rivera, 2011; Regalado and Ritter, 2016).

Fernandez et al. (2018) and Schunk et al. (2018) performed comparative analyses of fog water yields for different types of meshes in field conditions. Fernandez et al. (2018) used three one-square-meter fog collectors equipped with different meshes. The authors found that under similar wind conditions, the different kinds of fog collectors revealed inconsistent performance and lags in fog collection. Schunk et al. (2018) compared the water yield of 11 different meshes designed to enhance durability at high wind speed conditions. The authors found that monofilaments and three-dimensional meshes tend to show higher yields than the woven fabrics such as the Raschel mesh.

The comparative analyses of fog yields provide important knowledge about the relative difference in collection efficiency of various kind of meshes, at varying meteorological conditions. Such studies yield important contributions when it comes to selecting the best mesh for a particular site's meteorological conditions.

In field experiments, both meteorological conditions and fog characteristics varied during the events; in general, they differ from controlled conditions, as no steady state is achieved. Further, because the mesh has to reach saturation before the drainage process begins, a lag occurs between the arrival of the LWF to the collector and the beginning of collection (Fischer and Still, 2007; Fernandez et al., 2018). Because of fog's characteristics in these field conditions, we proposed the evaluation of collection efficiency during entire fog events.

Typically, fog collectors use a double Raschel mesh (Schemenauer et al., 1987, 1988; Cereceda et al., 2008; Schemenauer and Cereceda, 1991; Klemm et al., 2012; Marzol and Sánchez, 2008; Marzol, 2010;

Olivier, 2004). Nevertheless, other kinds of mesh have appeared on the market (Klemm et al., 2012) that could be (or already are) used to collect fog water. Because aerodynamic and deposition efficiencies depend on the mesh geometry and material, we expect different meshes to have varying collection efficiencies (Park et al., 2013; Fernandez et al., 2018; Schunk et al., 2018).

So far as we know, there are no published investigations into fog collection efficiency for entire fog events during field conditions. The goal of this study was to evaluate the fog collection efficiency η for entire fog events at field conditions. The analysis was performed using a standard fog collector (SFC) equipped with a square double Raschel mesh, 35% SC with an area of 1 m^2 , located 2 m agl. SFC is used worldwide to evaluate the potential of fog water collection (Schemenauer and Cereceda, 1994).

We defined fog collection efficiency as the ratio between CW and the unperturbed LWF normal to the collector's mesh, as integrated during entire fog events. The calculations were based on LWC measurements using a fog droplet spectrometer as well as measurements of wind speed and wind direction registered by a meteorological station located in El Sarco, a coastal site in the north of the semi-arid Coquimbo Region in Chile.

The paper starts by describing the study site, experimental set up and methodology before presenting and discussing the results. The results section includes an analysis of the microphysics of fog as well as a description of how fog collection efficiency depends on meteorological conditions and microphysics. The paper concludes with a summary and discussion of our findings.

2. Materials and methods

2.1. Study area

The study site is located in the northern coastal range in the semi-arid Coquimbo Region in Chile, south of the hyper-arid Atacama Desert and 43 km north of La Serena, the region's main city. The area is characterized by a complex topography, with increasing altitude to the east, reaching 1000 m in approximately 10 km. Along the coast, strong southerly winds following the terrain are observed (Rahn et al., 2011) that move eastwards during the day because of sea-land circulation (Montecinos et al., 2016). Rain precipitations are low and are characterized by high interannual variability. At the coast of the Coquimbo Region the mean precipitation is 100 mm year^{-1} , with a standard deviation of 60 mm year^{-1} (Bischoff-Gauss et al., 2006).

The experimental station is located on El Sarco Hill (29.51°S , 71.27°W and 700 m altitude), about 7 km from the coast. It is also 15 km south of El Tofo, where Schemenauer and Joe (1989) performed their experiments evaluating the fog collection efficiency of an LFC. Fig. 1 displays the study site, its location in Chile and the area's topography. The station is located in the saddle point of two mountains of roughly 1000 m above mean sea level. This placement forces the moist wind coming from the Pacific Ocean to converge on the site.

2.2. Experimental design

The experimental arrangement consists of a meteorological station equipped with sensors for wind speed and wind direction (Young, model 05106), temperature and relative humidity (RH) (Vaisala, model HMP155A) at 2.5 m and 10 m agl, and a rain gauge (Texas Electronics, model TE525MM-L25). Near the meteorological station, an SFC oriented in the SW direction (230°) was installed (Fig. 2). A second rain gauge measured the water collected by the SFC in multiples of 4.73 mL, the resolution of the rain gauge. Both meteorological data and collected water were registered every 3 sec and stored every 10 min. In our analysis, we only considered wind speed and wind direction data at 2.5 m agl and their relationship with the water collected by the SFC (CW).

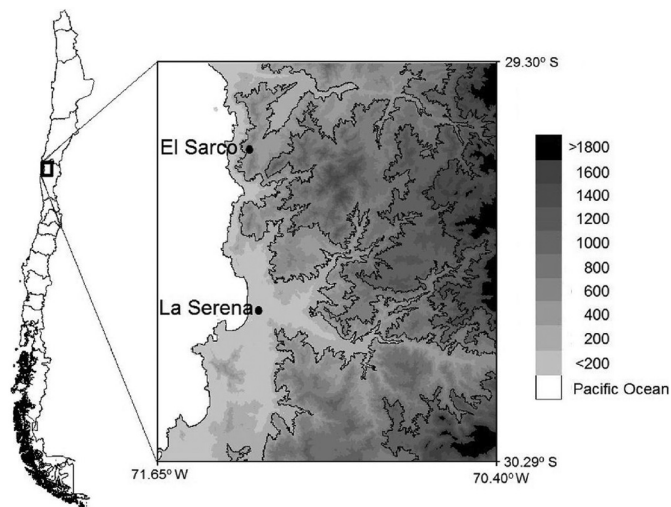


Fig. 1. Study site and its location in Chile. The grey scale at the right side represents the altitude in m. Contour lines are every 400 m.

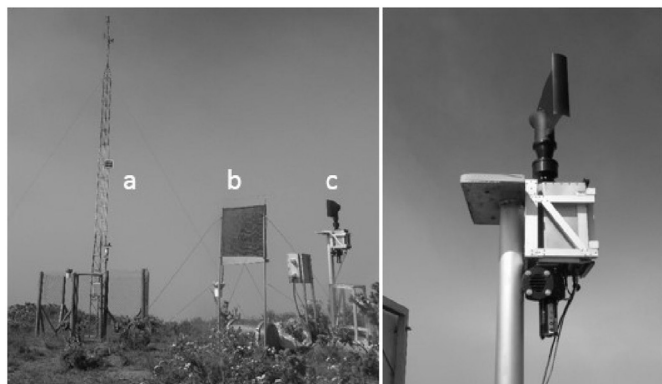


Fig. 2. Experimental design. Left: a: meteorological station, b: SFC and c: Fog monitor. Right: Zoom of the fog monitor

The LWC was evaluated using a Low Power Fog Droplet Spectrometer (LPFM-120) developed by Droplet Measurement Technologies, Boulder, USA. The device is a modified version of the fog monitor FM-120, adapted to work with 24V batteries, loaded with solar panels. A swivel head was connected to the fog monitor (FM), allowing the flux inlet to be oriented in the direction of the wind, as shown in Fig. 2. The FM detected the size distribution of aerosols in 30 bins between 2 μm and 50 μm in diameter. Data sampling and storage occurred every second.

The LWC was obtained in three-day field campaigns performed once per month, from January 2015 until March 2016. Because of instrument failures and/or absence of fog, the results shown in this article are based on data taken during the following periods:

- 19.01.2015 to 22.01.2015
- 23.02.2015 to 26.02.2015
- 28.07.2015 to 31.07.2015
- 05.01.2016 to 08.01.2016
- 02.02.2016 to 05.02.2016
- 08.03.2016 to 11.03.2016

We registered no rain precipitation for the analyzed events.

2.3. Evaluation of fog collection efficiency

In the case of planar fog collectors, efficiency is defined as the ratio

between the water collected by the gutter and the unperturbed LWF normal to the mesh achieving the collection surface of the SFC. The following applies:

$$\eta = \frac{CW}{\int_0^{\Delta t} \rho v \cos \beta A dt} * 100 \quad (1)$$

with CW being the collected water (kg) in the time interval Δt (s), ρ the LWC (kg m^{-3}), v (m s^{-1}) the unperturbed wind speed, β ($0 < \beta < 90^\circ$) the angle of incidence of the wind with respect to the normal (perpendicular) to the mesh, and A ($=1 \text{ m}^2$) the collector's area. The expression $\rho v \cos \beta$ is the projection of the liquid water flux (LWF) over the normal to the mesh.

For drainage to start, the mesh must be sufficiently wet, causing a lag between fog arrival and the start of the water harvest. Park et al. (2013) found that under controlled conditions (RH = 100%, temperature = 26.4 $^\circ\text{C}$; wind speed = 2 m s^{-1} ; droplet diameter = 6 μm), the collection efficiency of a Raschel mesh achieves a steady state just after four hours. At field conditions, fog events tend to differ in duration and meteorological conditions, and microphysical characteristics of fog changes continuously, so no steady state is achieved. Therefore, we considered the entire fog event to evaluate η ; in (1), Δt corresponds to the event's duration.

The LWC was calculated based on the size distribution of water droplets detected by the FM as follows:

$$\rho = \left(\sum_{j=1}^{30} N_j V_j \right) \rho_w, \quad (2)$$

here, N_j (m^{-3}) is the number of droplets in bin j during time interval Δt ; V_j (m^3) is the volume of the droplets in bin j ; and $\rho_w = 10^3 \text{ kg m}^{-3}$ is the density of liquid water.

The LWF integrated in the fog event was evaluated with LWC data, wind speed and wind direction, taking into account the mesh orientation. We evaluated the CW during the events using the registers of the pluviometer connected to the SFC. In this article, we define a fog event as having an LWC $\geq 0.01 \text{ g m}^{-3}$ based on the work of Gultepe et al. (2007). Additionally, because of wind direction errors, we only considered data for which wind speed was higher than 1 m s^{-1} when calculating η .

3. Results and discussion

3.1. Microphysics characteristics of fog

The LWC, averaged in 10-min intervals, achieved values of up to 1.45 g m^{-3} , and the MVD fluctuated between 5 μm and 28 μm . These results are similar to those obtained by Westbeld et al. (2009), Borys et al. (2009), and Schemenauer and Joe (1989).

Fig. 3 displays the relationship between LWC and MVD when LWC $\geq 0.01 \text{ g m}^{-3}$. As it can be observed in the figure, MVD increases with increasing LWC. This relationship can be explained because after (2), both LWC and MVD contains N_j and D_j raised to the same power. The linear regression that describes the relationship between MVD and LWC follows:

$$LWC = 0.04 \times MVD - 0.27 \quad (3)$$

with LWC in g m^{-3} and MVD in μm . The root mean square error for (3) is 2.5 μm ($R^2 = 0.6$).

The relationship between LWC and MVD also can be observed in Fig. 4, which displays the behavior of both variables for a sample of events. As previously stated, the behavior of both variables follows the same trend: an increase/decrease of LWC coincides with an increase/decrease of MVD.

Fog events differed in duration, microphysical characteristics and atmospheric parameters. As indicated by the 10-min data, the average LWC over entire fog events increases with the average MVD (not

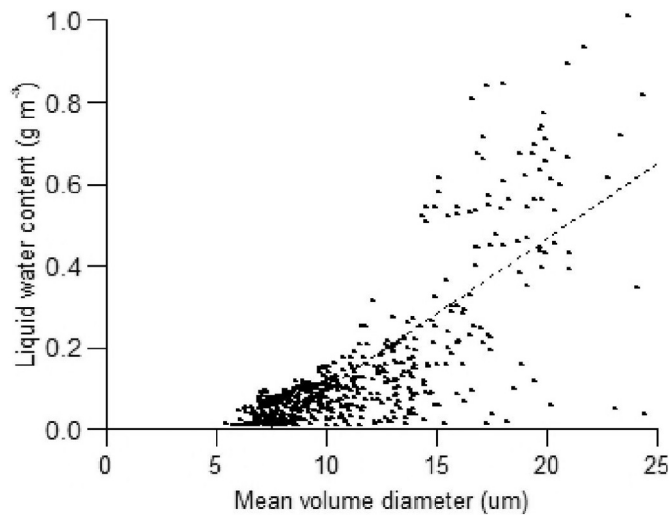


Fig. 3. Dependence of LWC on MVD. The points corresponds to 10-min data

shown).

Fig. 5 displays the size and LWC spectral distribution of the events marked in Fig. 4 as a, b and c, which are representative of the spectral distribution of the events shown in Table 1. We can observe that LWC and size presents maximum values at different bins because LWC depends on the volume of the droplet's diameter. The mean LWC in events a, b and c were 0.04 g m^{-3} , 0.65 g m^{-3} and 0.55 g m^{-3} , respectively, with corresponding MVD values of $8.6 \text{ }\mu\text{m}$, $20.2 \text{ }\mu\text{m}$ and $24.2 \text{ }\mu\text{m}$.

3.2. Fog collection efficiency

Fig. 6 shows the behavior of LWF and CW in a sample of events. As a reference, the LWC values are presented as well. We would like to emphasize that fog was present ($\text{LWC} \geq 0.01 \text{ g m}^{-3}$) in some cases;

however, the LWF cannot be evaluated because the wind speed was less than 1 m s^{-1} due to a wind direction error (for example in graph C).

As the graphs in Fig. 6 illustrate, the relationship between the behavior of LWF and CW depends on the event:

- Fog events without measured water output ($\text{CW} = 0$) were observed. Examples are A1 and C5. As explained in Section 3.2, the mesh requires saturation to begin the draining process. If this condition is not reached, no water can be harvested.
- When water is harvested, there was a lag between the fog's arrival and the beginning of measured water output at the SFC. This lag ranged from zero (event F12) and one hour (events C6 and E10). Both processes began simultaneously when preceded by another fog event. Water harvesting and fog arrival can begin simultaneously if the mesh is already saturated due to a preceding fog event.
- In some cases, water collection continued for one hour after the end of the event. Examples are events B3, D9 and E10. These cases are explained by the fact that the mesh continues to hold water even once the fog event finishes. Depending on the evaporation rate, the draining process continues until there is no more water to drain.
- There were cases in which the CW was greater than the LWF incident. Examples include Fa, Fc and Fb (partially), where it occurred at the beginning of the event. This finding could be related to the water collection of drizzle. In fact, the vertical speed of drizzle droplets with diameters less than $150 \text{ }\mu\text{m}$ is less than 0.5 m s^{-1} (Holtermann, 2003). When the wind speed is above 2 m s^{-1} , the droplets move almost horizontally, therefore making them undetectable by the meteorological station's rain gauge. It is important to note that the FM does not detect drizzle due to its droplet range diameter. It is very difficult and expensive to measure drizzle, and it is beyond the scope of this paper.

To evaluate η , we analyzed 34 fog events, excluding events in which CW was higher than LWF. Table 1 shows the η for the 27 remaining events. It also includes the following information: the initial time,

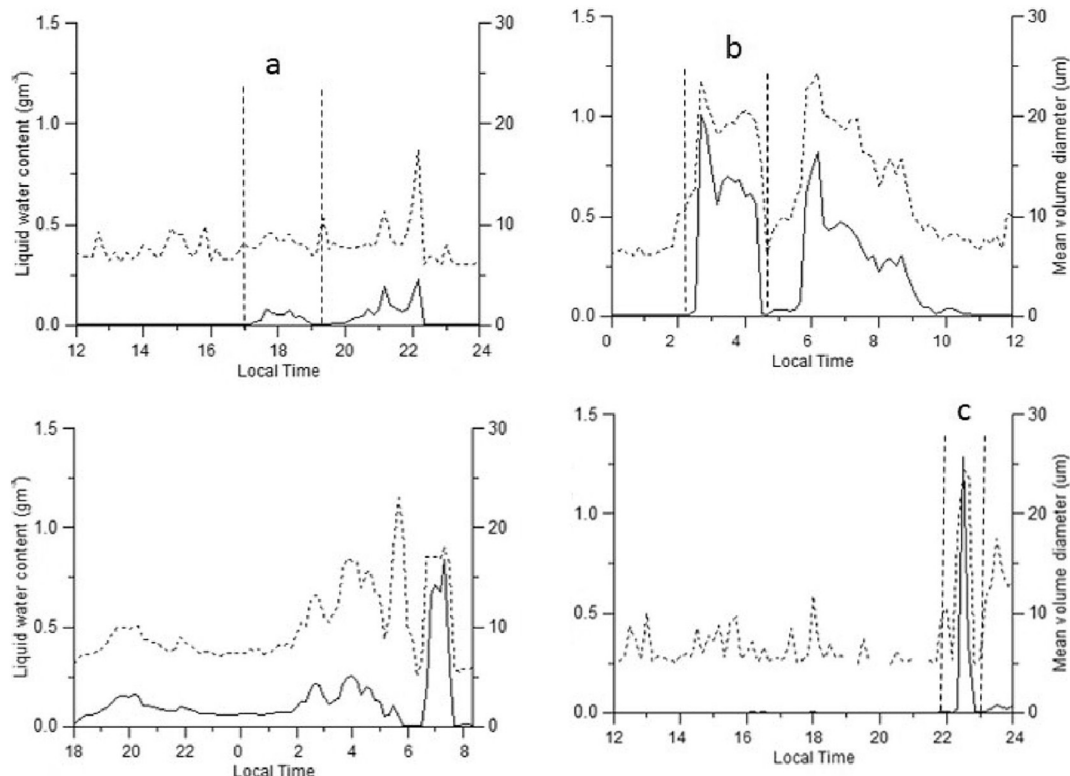


Fig. 4. LWC (solid) and MVD (dotted) observed in a sample of fog events. a: January 20, 2015; b: January 21, 2015; c: February 24/25, 2015; d: July 29, 2015.

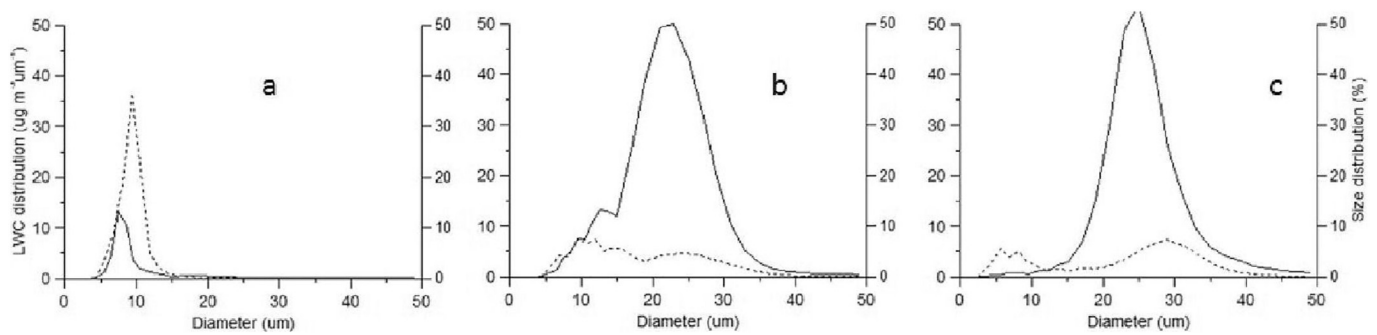


Fig. 5. LWC (solid) and size (dashed) spectral distribution in 3 fog events; a: January 20, 2015, from 1200 LT to 2400 LT; b: January 21, 2015, from 0220 LT to 0420 LT; c: July 29, 2015, from 2210 LT to 2240 LT.

Table 1

Mesh Collection Efficiency (MCE), initial time (Date and time in LT), duration of the event (Dt), wind speed (V), DPD, LWC and MVD averaged for each fog event.

N	Initial time	Dt	η	V	DPD	LWC	MVD
	yyymmdd hh:mm	Minutes	%	m s^{-1}	$^{\circ}\text{C}$	g m^{-3}	μm
1	150120 17:10	100	0.0	5.7	0.21	0.044	8.4
2	150120 19:40	150	4.8	3	0.08	0.082	9.3
3	150121 02:20	100	11.8	1.9	0.1	0.659	19.4
4	150121 04:50	300	14.7	2.2	0.02	0.274	15.0
5	150121 13:40	100	0.0	7.1	0.41	0.044	8.8
6	150121 17:00	100	8.7	8.8	0.18	0.062	8.3
7	150121 19:10	150	22.4	4.1	0.04	0.225	11.8
8	150121 23:40	50	9.4	1.2	0.02	0.35	19.1
9	150122 02:10	410	20.3	1.8	0.02	0.392	14.9
10	150223 17:40	700	36.8	3	0.03	0.103	9.5
11	150729 22:10	20	0.0	1.3	2.75	0.654	21.3
12	150730 08:20	80	20.4	4.7	0.03	0.05	7.0
13	150730 14:50	70	19.7	4.9	0.08	0.065	7.8
14	150730 16:10	20	0.0	2	0.32	0.072	11.7
15	150730 16:40	120	36.2	3.9	0.06	0.085	8.7
16	160106 03:30	50	0.0	2.2	0.16	0.069	9.0
17	160106 04:20	30	19.7	3.2	0.1	0.072	8.8
18	160106 05:40	30	32.4	1.4	0.08	0.068	9.8
19	160107 00:40	20	0.0	2.2	0.17	0.024	7.4
20	160202 20:10	150	19.4	3.3	0.13	0.07	7.1
21	160203 05:40	60	0.0	1.8	0.13	0.061	11.5
22	160203 07:40	110	0.0	2.6	0.16	0.095	10.6
23	160203 17:30	40	0.0	5.9	0.25	0.027	7.3
24	160203 20:00	90	0.0	2.6	0.16	0.029	6.9
25	160205 06:50	20	0.0	2.5	0.24	0.027	9.7
26	160309 23:50	30	0.0	1.5	0.65	0.07	11.8
27	160310 00:40	30	0.0	1.8	0.72	0.158	16.3

duration of the event (Dt), and average values of wind speed (V), DPD, LWC and MVD for each fog event. A number identifying the event (first column) corresponds to the same number displayed in the individual graphics of Fig. 6. We found that η ranged between 0% and 36.8%. The event with the highest value of η happened in February, 2015 (10 in Table 1, E10 in Fig. 6).

From all the cases, those with a duration of up to 30 minutes CW was zero (events 11, 14, 19, 25, 26 and 27 in Table 1), except if preceded by another fog event (events 17 and 18 in Table 1). As mentioned before, this lag occurs because the mesh requires time to become saturated enough to start dripping. Further, for events longer than 30 minutes, η equals zero if the mean DPD > 0.2 °C (Fig. 7, left) or the mean LWC < 0.045 g m^{-3} (not shown). This fact can be explained because (1) high DPD values are related to low RH values. Although fog can occur for values as low as 50% RH (Lamb and Verlinde, 2011), in such cases mesh saturation could take longer than for higher RH; and (2) low LWC values are related to low LWF, requiring more time for mesh saturation. Nevertheless, there were also events without fog water collection that not satisfied the above conditions. The figure also

suggests that for DPD < 0.2 °C, the maximum η increases with a decrease in DPD. However, the number of data points are not enough to be conclusive and more field experimental needs to be made.

The right panel of Fig. 7 displays the relationship between η and number concentration (Nc). Hereinafter, events with LWC < 0.045 g m^{-3} or DPD > 0.2 °C are not displayed. The figure shows that for Nc between 180 cm^{-3} and 260 cm^{-3} , η is independent from Nc. For Nc > 260 cm^{-3} , the values are all above 20%, and no clear relationship between η and Nc can be observed.

The left panel of Fig. 8 shows the dependence of η on wind speed. In the graph, we distinguish cases of MVD below and above 12 μm . If all events are considered, no clear relationship between both variables can be observed. However, an increase of η with wind speed exists for those events in which MVD $\geq 12 \mu\text{m}$ (squares). Below this value, there exists no clear relationship between the variables. The behavior of η for MVD $\geq 12 \mu\text{m}$ could result primarily from the deposition mechanism whose efficiency increases with wind speed until reaching a certain threshold (Regalado and Ritter, 2016). For MVD < 12 μm , aerodynamic efficiency - which is independent of wind speed - (see Rivera, 2011 for details) could be the most relevant mechanism for fog collection.

The relationship between η and MVD is displayed in the right panel of Fig. 8. Discarding the events with MCE = 0%, for MVD $\geq 10 \mu\text{m}$, a decrease of η occurs with an increase of MVD. Below this value, no dependence appears between the variables. Both graphics in Fig. 8 may be related because big droplets are usually formed with low wind speed. In fact, after observations performed by the authors based on 10-min data, droplets with MVD $\geq 12 \mu\text{m}$ appeared only for wind speeds lower than 6 m s^{-1} . Further, we found that for wind speeds below 4 m s^{-1} , the maximum MVD increases with decreasing wind speed (not shown). The decreasing of η with MVD for MVD $\geq 10 \mu\text{m}$ could be related to fog droplet blow-off and bounce-off, phenomena hypothesized by Thorne et al. (1982) under controlled conditions.

Though the definition of collection efficiency used in this work differs from that of Schemenauer and Joe (1989), we can point to some similarities in findings. The authors found that a) efficiency (E_m) increases with wind speed for MVD near 15 μm , and b) E_m decreases with increased MVD. We remark that because the authors measured LWC behind and in front of the LWC, the draining process was not considered when evaluating E_m .

4. Conclusions

Fog collection represents a sustainable and effective alternative water source in many parts of the world. In the past three decades, major advances have been made regarding fog characterization, geographical identification, and collector design. Nonetheless, there remains little information about the collection efficiency of these devices. Collection efficiency is one of the most important parameters affecting the final cost of water produced by fog projects (LeBoeuf and de La

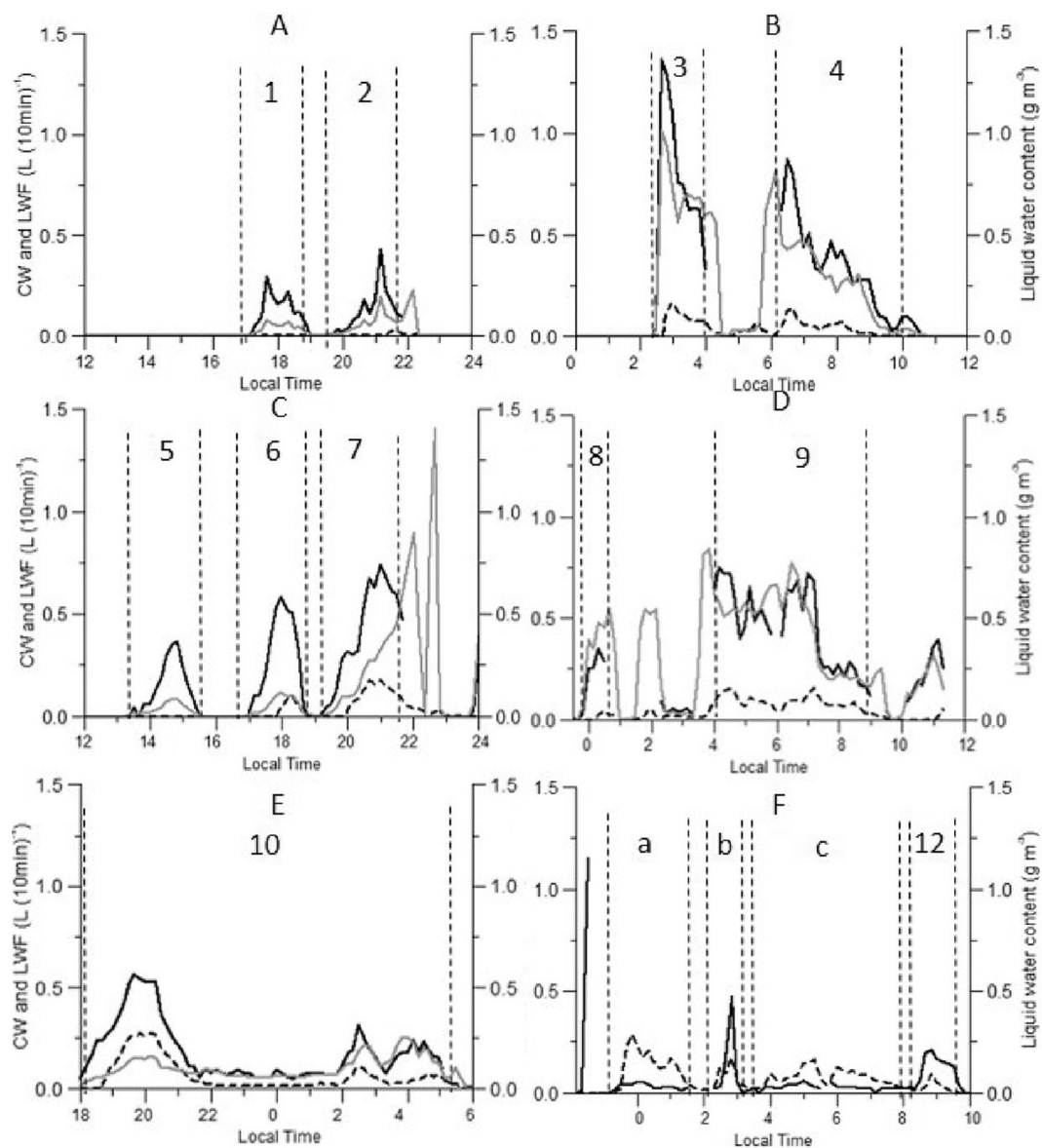


Fig. 6. LWF (solid black), collected water output (dotted) and LWC (solid, grey). A: January 20, 2015; B: January 21, 2015; C: January 21, 2015; D: January 22, 2015; E: February 23, 2015; F: July 29/30, 2015.

Jara, 2014). Therefore, it is of utmost importance the study of fog collection efficiency and its dynamics at field conditions.

This work analyzed the fog collection efficiency of a SFC equipped with a Raschel mesh. Three-day field campaigns were performed from January 2015 to March 2016 in El Sarco, a hill on the coastal range of

the semi-arid Norte Chico of Chile. A fog droplet spectrometer was used to measure the size distribution of fog droplets, which was used to calculate LWC. The collection efficiency η was calculated dividing the water collected by the gutter and the LWF accumulated during entire fog events. We considered entire fog events because a steady state is

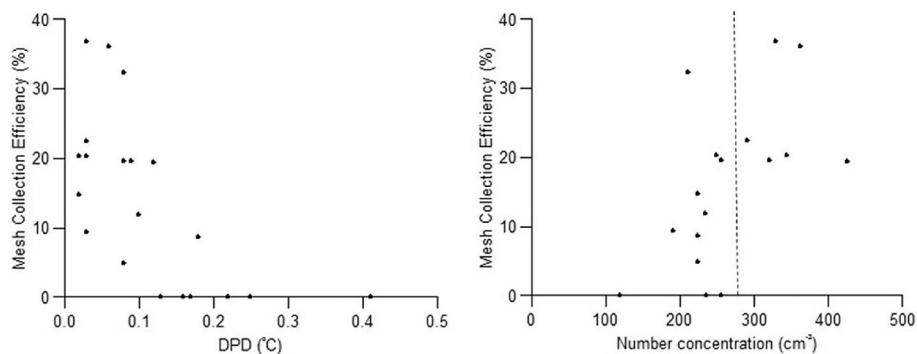


Fig. 7. Mesh collection efficiency and DPD (left) and number concentration (right).

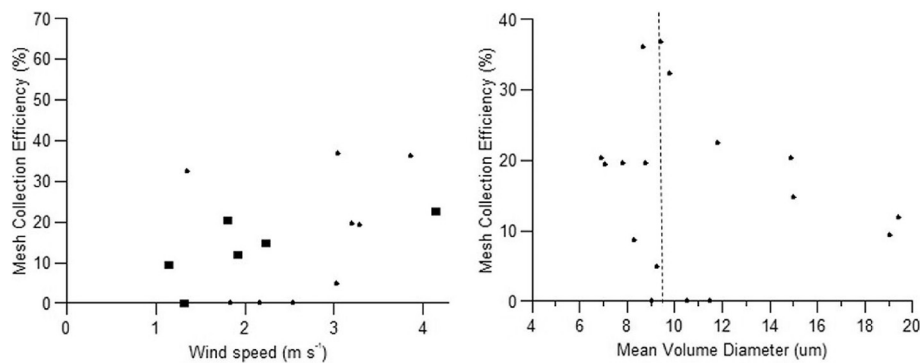


Fig. 8. Left: Mesh collection efficiency and wind speed. Squares and points represent events with values of MVD ≥ 12 and MVD < 12 μm , respectively. Right: Mesh collection efficiency and MVD. The vertical line separates the cases MVD lesser and larger than ~ 10 μm .

generally not achieved during field conditions. In addition, there is usually a lag between the fog's arrival and the start of collection.

We defined fog as $\text{LWC} \geq 0.01 \text{ g m}^{-3}$ (Gultepe et al., 2007). In this range, we found that LWC increases with higher MVD for both 10-min data and for values averaged over entire fog events.

The duration of the events was between 20 min and 11 h 40 min. We found that the collection efficiency ranged between 0% and 36.8%. Events lasting less than 30 min did not register collected water, unless preceded by another fog event, which can be explained because the mesh requires saturation to start dripping. The dripping process can continue for one hour after the end of the fog event because once the fog event has finished, the mesh is still wet, allowing the draining process to continue.

We found a complex interdependence between fog collection, microphysics and meteorological conditions. For the studied events, no water collection was registered when the mean DPD was above 0.2 $^{\circ}\text{C}$ or when the mean LWC was below 0.045 g m^{-3} . For N_c between 180 cm^{-3} and 260 cm^{-3} , η was independent from N_c . Further, for MVD above $10 \mu\text{m}$, there was a decrease of η with an increase of MVD. This finding could result from fog droplet blow-off and bounce-off.

For MVD larger than $12 \mu\text{m}$, η increases with wind speed. In other cases (MVD $< 12 \mu\text{m}$), the dependence of η on MVD does not show clear patterns.

We highlight that though this research did not consider the full diversity of events that can occur in field conditions, it still provides information about fog collection efficiency and its relationship with meteorological variables and microphysics characteristics.

Acknowledgments

This research was funded by Project Dominga of Andes Iron, SpA, and partially supported by CONICYT FONDECYT through grant 11140863. It is attached to the Plan de Mejoramiento Institucional en Eficiencia Energética y Sustentabilidad Ambiental ULS-1401.

References

Bischoff-Gauss, I., Kalthoff, N., Fiebig-Wittmaack, M., 2006. The influence of a storage lake in the Arid Elqui Valley in Chile on local climate. *Theor. Appl. Climatol.* 85, 227–241.

Borys, R.D., Lowenthal, D.H., Wetzel, M.A., Herrera, F., Gonzalez, A., Harris, J., 2009. Chemical and microphysical properties of marine stratiform cloud in the North Atlantic. *J. Geophys. Res.* 114, 22073–22085.

Cereceda, P., Larrain, H., Farias, M., Egaña, I., 2008. The spatial and temporal variability of fog and its relation to fog oases in the Atacama Desert. *Chile. Atmos. Res.* 87, 312–323.

Fernandez, D.M., Torregrosa, A., Weiss-Penzias, P.S., Zhang, B.J., Sorensen, D., Cohen, R.E., McKinley, G.H., Kleingartner, J., Oliphant, A., Bowman, M., 2018. Fog water

collection effectiveness: mesh intercomparisons. *Aerosol Air Qual. Res.* 18, 270–283.

Fischer, D.T., Still, C.J., 2007. Evaluating patterns of flow water deposition and isotopic composition on the California Channel Islands. *Water Resour. Res.* 43, 1944–1973.

Gultepe, I., Tardif, R., Michaelides, C., Cermak, J., Bott, A., Bendix, J., Müller, D., Pagowski, M., Hansen, B., Ellrod, G., Jacobs, W., Toth, G., Cober, G., 2007. Fog research: a review of past achievements and future perspectives. *Pure Appl. Geophys.* 164, 1121–1159.

Holtermann, H.J., 2003. Kinetics and evaporation of water drops in air, IMAG report 2003-12. Wageningen UR.

Klemm, O., Schemenauer, R.S., Lummerich, A., Cereceda, P., Marzol, V., Corell, D., van Heerden, J., Reinhard, D., Gherezghier, T., Olivier, J., Osses, P., Sarsour, J., Frost, E., Estrela, M.J., Valiente, J.A., Fessehay, G.M., 2012. Fog as a fresh-water resource: overview and perspectives. *Ambio* 41, 221–234.

Lamb, D., Verlinde, J., 2011. *Physics and Chemistry of Clouds*. Cambridge University Press.

LeBoeuf, R., de la Jara, E., 2014. Quantitative goals for large-scale fog collection projects as a sustainable freshwater resource in northern Chile. *Water Int.* 39, 431–450.

Marzol, M.V., 2010. Historical background of fog water collection studies in the Canary Islands. In: Bruijnzeel, L., Scatena, F., Hamilton, L. (Eds.), *Tropical Montane Cloud Forests: Science for Conservation and Management*, pp. 352–358.

Marzol, M.V., Sánchez, J., 2008. Fog water harvesting in Ifni, Morocco. In: *An Assessment of Potential and Demand*. 139. *Die Erde, Zeitschrift der Gesellschaft für Erdkunde zu Berlin*, pp. 97–126.

Montecinos, S., Gutiérrez, J.R., López-Cortés, F., López, D., 2016. Climatic characteristics of the semi-arid Coquimbo Region in Chile. *J. Arid. Environ.* 126, 7–11.

Olivier, J., 2004. Fog harvesting: An alternative source of water on the west coast of South Africa. *Geo J.* 6, 203–221.

Park, K., Chhatre, S.S., Srinivasan, S., Cohen, R.E., 2013. Optimal design of permeable fiber network structures for fog harvesting. *Langmuir* 29, 13262–13277.

Rahn, D.A., Garraud, R., Rutllant, J., 2011. The low-level atmospheric circulation near Tongoy Bay–Point Lengua de Vaca (Chilean Coast, 30°S). *Mon. Weather Rev.* 139, 3628–3647.

Regalado, C.M., Ritter, A., 2016. The design of an optimal fog water collector: a theoretical analysis. *Atmos. Res.* 178–179, 45–54.

Rivera, J., 2011. Aerodynamic collection efficiency of fog water collectors. *Atmos. Res.* 102, 335–342.

Schatzmann, M., 1999. Wind tunnel modelling of fog droplet deposition on cylindrical obstacles. *J. Wind Eng. Ind. Aerod.* 83, 371–380.

Schemenauer, R.S., Cereceda, P., 1991. Fog-water collection in arid coastal locations. *Ambio* 20, 303–308.

Schemenauer, R.S., Cereceda, P., 1994. A proposed standard fog collector for use in high-elevation regions. *J. Appl. Meteor.* 33, 1313–1322.

Schemenauer, R.S., Joe, P.I., 1989. The collection efficiency of a massive fog collector. *Atmos. Res.* 24, 53–69.

Schemenauer, R.S., Cereceda, P., Carvajal, N., 1987. Measurements of fog water deposition and their relationships to terrain features. *J. Clim. Appl. Meteorol.* 26, 1285–1291.

Schemenauer, R.S., Fuenzalida, H., Cereceda, P., 1988. A neglected water resource: the Camanchaca of South America. *Bull. Am. Meteorol. Soc.* 69, 138–147.

Schuck, C., Trautwein, P., Hruschka, H., Frost, E., Dodson, L., Derhem, A., Bargach, J., Menzel, A., 2018. Testing water yield, efficiency of different meshes and water quality with a novel fog collector for high wind speeds. *Aerosol Air Qual. Res.* 18, 240–253.

Thorne, P.G., Lovet, G.M., Reiners, W.A., 1982. Experimental determination of droplets' impact on canopy components of balsam fir. *J. Appl. Meteor.* 21, 1413–1416.

Westfeld, A., Klemm, O., Griessbaum, F., Sträter, E., Larrain, H., Osses, P., Cereceda, P., 2009. Fog deposition to a Tillandsia carpet in the Atacama Desert. *Ann. Geophys.* 27, 3571–3576.